Case Studies in Thermal Engineering 35 (2022) 102111

Contents lists available at ScienceDirect

Case Studies in Thermal Engineering

journal homepage: www.elsevier.com/locate/csite

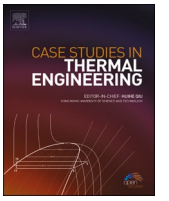

Equivalent temperature prediction for concrete-filled cold-formed steel (CF-CFS) built-up column sections (part B)

Rohola Rahnavard [*], Hélder D. Craveiro [**], Rui A. Simões, Aldina Santiago

University of Coimbra, ISISE, Department of Civil Engineering, Coimbra, Portugal

ARTICLE INFO

Keywords:
Concrete inner core
Concrete outer core
Equivalent temperature
Embedded steel area
Heat transfer analysis

ABSTRACT

Innovative concrete-filled cold-formed steel (CF-CFS) built-up column sections subjected to axial compression and elevated temperatures were previously investigated, assessing their structural fire performance. However, the analytical fire resistance methodology presented in the EN1994-1-2 requires advanced heat transfer analysis to compute the temperature evolution of the steel and concrete components of the composite cross-section. This paper presents a set of empirical formulations to predict equivalent temperature for steel and concrete components of CF-CFS built-up column sections. The finite element modeling technique to predict temperature evolution through the CF-CFS built-up column sections was calibrated using a 2-D heat transfer analysis (part A of this study). As a simplification, the concrete infill was divided into two areas, namely inner and outer core areas. The equivalent temperature of the steel section and the steel embedded area were also considered. The results showed good accuracy of the proposed empirical formulas.

Notation

H	Height of the cross-section
B	Width of the cross-section
L	Distance of the embedded steel surface to the section surface subjected to radiation
T	Standard temperature (°C)
T_0	Initial temperature (°C)
C, R, and M	Constant parameters
$A_{in.con\ core}$	Area of inner concrete core (mm^2)
$A_{total.con\ core}$	The total area of the concrete (mm^2)
$A_{total.comp}$	The total area of the composite cross-section (mm^2)
h_u	Height of the U-shaped profile (mm)
b_u	Flange width of the U-shaped profile (mm)
h_c	Height of the C-shaped profile (mm)
b_c	Flange width of the C-shaped profile (mm)
c_c	Lip length of the C-shaped profile (mm)

* Corresponding author.
** Corresponding author.
E-mail addresses: rahnavard@uc.pt, rahnavard1990@gmail.com (R. Rahnavard), heldercraveiro.eng@uc.pt (H.D. Craveiro).

https://doi.org/10.1016/j.csite.2022.102111
Received 13 April 2022; Received in revised form 6 May 2022; Accepted 7 May 2022
Available online 12 May 2022

t_s	CFS profile thickness
$t_{s,emb}$	Summation of the embedded steel thicknesses (mm)
t	Time (h)
$\widetilde{d}$	Equivalent thickness of concrete
$\widetilde{t}_s$	equivalent thickness of steel
c_p	Specific heat
θ_{eq}	Equivalent temperature
α	Cronbach's alpha

1. Introduction

Due to its superior structural performance in various circumstances, concrete-filled steel tube (CFST) composite columns are widely used in various structures. Moreover, because the thermal conductivity and specific heat of concrete are low, it can improve the fire behavior of composite columns. Cold-formed steel profiles have several advantages over those hot rolled, including shorter construction time, economic efficiency, and accessible transportation [1-14]. Extensive experimental, computational, and analytical research has been undertaken over the last decades to understand better the behavior of composite columns exposed to fire [15-26]. A

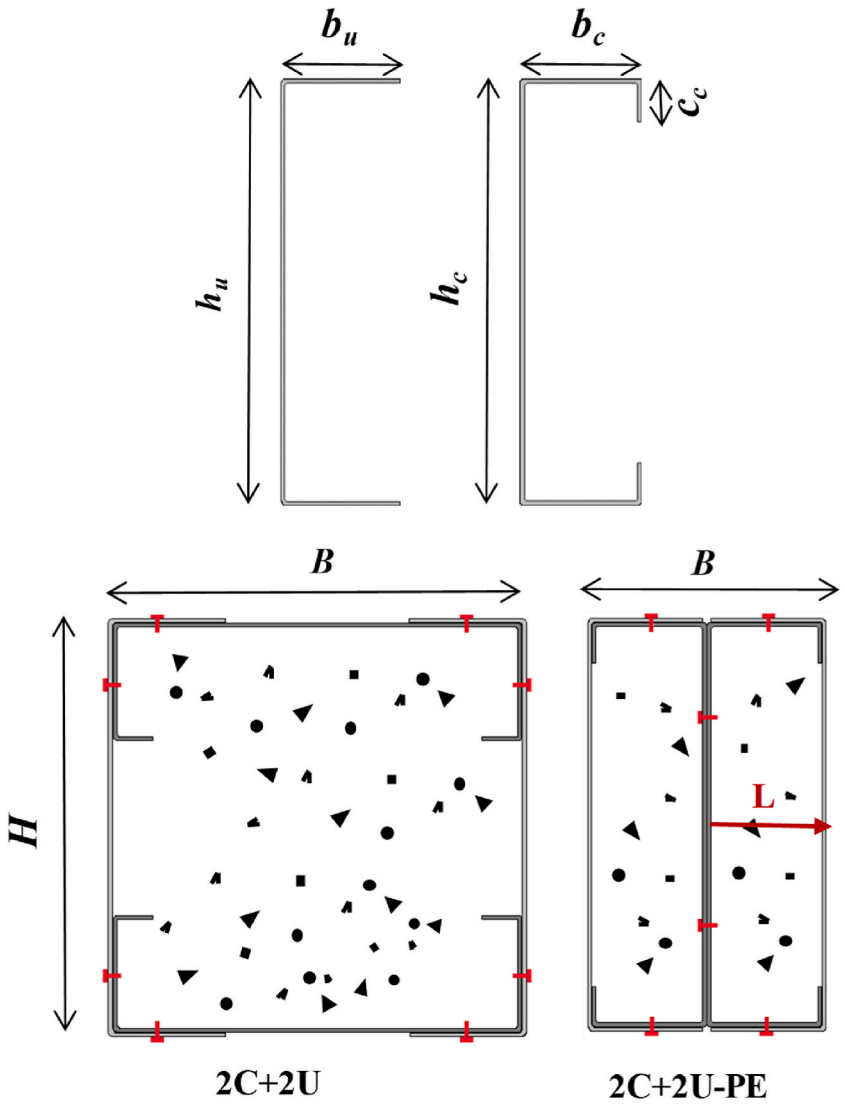

Fig. 1. Geometry of CFS profiles and CF-CFS built-up sections.

simple design approach for CFST columns in a fire was provided by Ukanwa et al. [19-22]. The suggested design technique was provided for square, rectangular, and circular columns based on equivalent temperatures and equivalent strength for the cross-sectional components. Yu et al. [23-26] experimentally and numerically measured the fire resistance of a series of CFST composite columns. They recommended modifying EN 1994-1-2 [27] by considering equivalent temperatures of steel and concrete components and applying them to the overall formulation. According to their findings, the equivalent temperatures approach for measuring fire resistance of CFST columns with various section profiles predicts with reasonable accuracy.

Although experimental, numerical, and analytical studies on temperature evolution and fire resistance of concrete-filled steel tube composite columns were performed, no research was presented on concrete-filled built-up cold-formed steel composite sections. The EN1994-1-2 [27] presents two design methods, namely the general and simplified methods. Both methods require advanced heat transfer analysis to assess the temperature evolution in different concrete depths. Performing heat transfer analysis, especially for CF-CFS profiles, required a good knowledge of finite element analysis, thermal properties, and heat transfer analysis. Additionally, a precise definition is necessary to achieve an accurate result. The authors presented a 2D finite element approach in Part A [28] of the current study and calibrated it using the available experimental data presented in Ref. [16]. This paper proposes simplified empirical formulas to predict the equivalent concrete and steel temperature. The results were compared with ones obtained from heat transfer analysis. These simplified empirical formulas aim to present a methodology independent of finite element analysis. Moreover, by predicting an equivalent temperature of steel and concrete, common complex calculations in the EN1994-1-2 [27] can be simplified because the number of temperature layers is reduced dramatically.

2. Description of the CF-CFS built-up sections

The discussion on the application and design procedure for the CF-CFS built-up section is available in Ref. [28]. In this study, the cold-formed steel profiles, including C, and U-shaped, were considered for the built-up sections, as shown in Fig. 1. The thickness of the CFS profiles included 1.5 mm and 3 mm. The geometry of two CF-CFS cross-sections is presented in Fig. 1. The considered sections in this study were according to the limitation of EN1993-1-3 [29] for the cold-formed steel profiles. The geometry details of the CF-CFS sections are listed in Table 1. Two configurations were considered in this study, are named:

a) Concrete-filled CFS built-up cross-section comprising two C-shaped profiles and two U-shaped profiles (2C+2U),
b) Concrete-filled CFS built-up cross-section (partially embedded) comprising two C-shaped profiles fastened back-to-back and two U-shaped profiles (2C+2U-PE).

The paper investigates 74 CF-CFS built-up composite sections, including 54 sections for 2C+2U and 18 sections for 2C+2U-PE.

3. Numerical modeling and results

3.1. Modeling assumptions

All CF-CFS built-up composite sections explained in Section 2 were modeled using the finite element method software Abaqus [30]. The modeling techniques were calibrated against experimental results conducted by Rahnavard et al. [16] and are detailed in Part A of this study [28]. DC2D4 element type with a size of 0.5 was selected according to the calibration available in Ref. [28]. However, it should be mentioned that the mesh size doesn't significantly affect the results. The heat conductance for the contacts between concrete and steel was assumed as 200 W/m^2 K [16,28]]. For the case of steel to steel contacts, the value 2000 W/m^2 K was considered. The resultant heat emissivity of 0.23 was selected to define radiation. The convective heat coefficient also was taken as 25 (W/m^2 K) according to EN 1991-1-2 [31] to define convection. Note that thermal amplitude for radiation and convection in this parametric study was adopted from ISO 834 [32]. The standard temperature (T) vs. time (t) curve of ISO 834 is obtained from Eq. (1), where T_0 is the initial temperature (°C) and is equal to 20 °C.

$$T = T_0 \times 345 \log_{10}(8t + 1) \tag{1}$$

3.2. Temperature evolution

The temperature evolution of the different 2C+2U-PE sections is presented in Fig. 2. As can be observed, there is a minor

Table 1
CFs profile details.

Section	U-shaped				C-shaped				
	h_u (mm)	b_u (mm)	t_s (mm)	b_u/t	h_c (mm)	b_c (mm)	c_c (mm)	t_s (mm)	b_c/t
2C+2U	153	44.5	1.5	28.6	150, 200, 300	43, 60, 75	15.0	1.5	28.6, 40, 50
	159	46.0	3.0	15.3	153, 203, 303	46, 60, 75	16.5	3.0	14.3, 20, 25
	200	44.5	1.5	28.6	150, 200, 300	43, 60, 75	15.0	1.5	28.6, 40, 50
	206	46.5	3.0	15.3	153, 203, 303	46, 60, 75	16.5	3.0	14.3, 20, 25
	300	44.5	1.5	28.6	150, 200, 300	43, 60, 75	15.0	1.5	28.6, 40, 50
	306	46.5	3.0	15.3	153, 203, 303	46, 60, 75	16.5	3.0	14.3, 20, 25
2C+2U-PE	153, 203, 303	44.5, 61.5, 76.5	1.5	28.6, 41, 51	150, 200, 300	43, 60, 75	15.0	1.5	28.6, 40, 50
	159, 209, 309	44.5, 61.5, 76.5	3.0	28.6, 41, 51	153, 203, 303	43, 60, 75	15.0	3.0	28.6, 40, 50

temperature difference between the cross-section center and half of the cross-section dimensions (H/2 and B/2). Therefore, the next goal is to provide an empirical formulation to predict the equivalent temperature for the concrete inner core with dimensions of $B/2 \times H/2$ and concrete outer core. This strategy can contribute to simplifying the application of existing design formulations to conduct safety verification of composite columns in fire.

4. Analytical procedure

4.1. Introduction

This section details the empirical formulation used for calculating the equivalent temperature as a function of time for concrete and steel components of CF-CFS built-up composite sections. The following section presents the formulas for two concrete areas, including inner and outer cores, according to the observation from Section 3.2.

4.2. Concrete equivalent temperature

Yu et al. [24] presented an empirical formulation using the finite element method and nonlinear regression analysis to calculate steel and concrete equivalent temperatures. The formula validated solid and hollow concrete-filled tubular steel composite columns with circular and polygonal sections. This paper adopts and modifies the empirical formula presented by Yu et al. [24] for CF-CFS built-up composite sections.

The concrete section was divided into two parts, including inner and outer cores. For the concrete-filled cold-formed steel composite section with no embedded steel region (2C+2U), the equivalent temperature of concrete for both inner and outer concrete cores is calculated using Eq. (2), where t is the fire exposure time in hours, and R is obtained from Eq. (3). In Eq. (3), the parameter $\widetilde{d}$ is the equivalent thickness of concrete in meters calculated based on Eq. (4). The parameters α and β are obtained from Eqs (5) and (6), respectively. In Eqs (5) and (6), B and H are the section dimensions (in mm). In Eq. (2), the parameter M is obtained from Eq. (7), where $\widetilde{t}_s$ is the equivalent thickness of steel (in meters) and can be obtained from Eq. (8). In Eq. (2), the parameter C is selected based on Eq. (9).

The equivalent temperature of concrete for the inner concrete core of the CF-CFS composite section with the embedded steel area

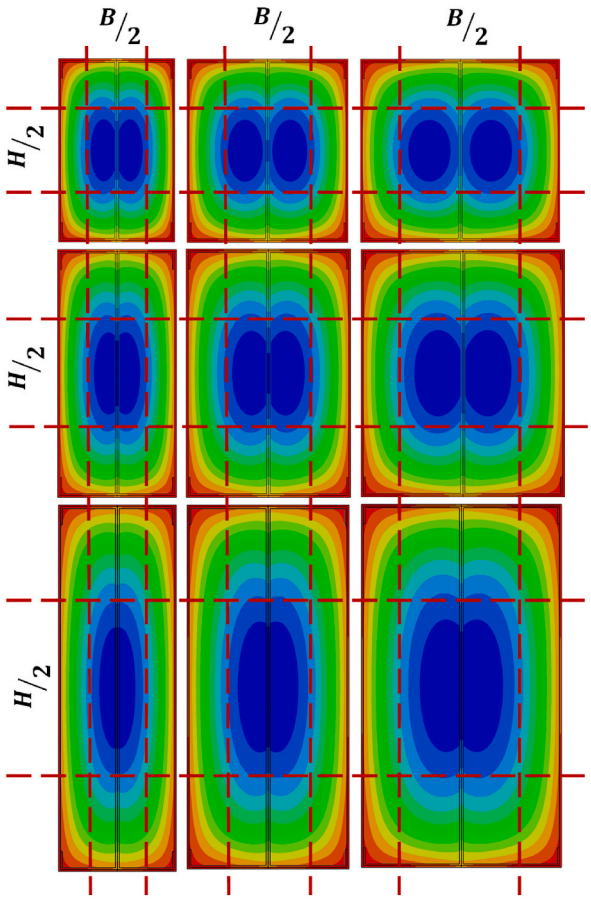

Fig. 2. Temperature evolution of the different 2C+2U-PE sections.

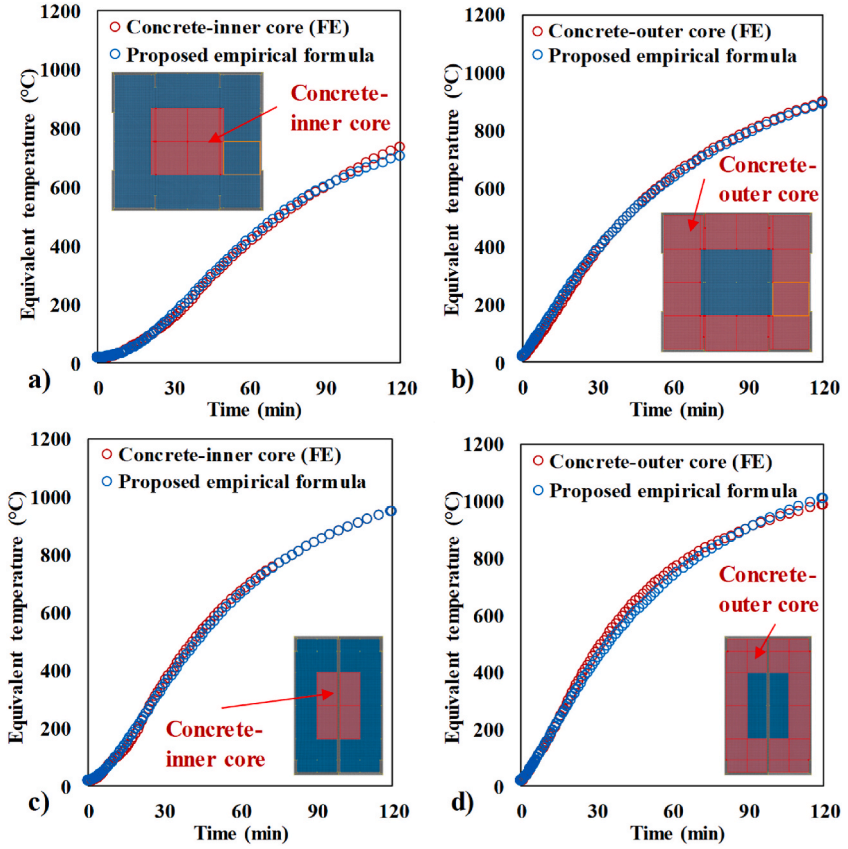

Fig. 3. Equivalent temperature history for concrete; a) inner core (2C+2U) b) outer core (2C+2U), c) inner core (2C+2U-PE), and d) outer core (2C+2U-PE).

(2C+2U-PE) is determined using the same procedure explained for the one with no embedded steel area (2C+2U), while β is 25 and α is calculated according to Eq. (10). Moreover, the C parameter for the inner core is 1.65 when the minimum dimension of the cross-section is less than 100 mm; otherwise, it is 1.9.

$$\theta_{eq} = 2R\left(1 - \frac{1}{1 + \left(t/M\right)^{C}}\right) + 20 \tag{2}$$

$$R = 120 + \left(\alpha e^{-\beta \widetilde{d}}\right) \tag{3}$$

$$\widetilde{d} = \begin{cases} \sqrt{A_{in,con\ core} \times 10^{-6}/\pi} & for\ inner\ concrete\ core \\ \sqrt{A_{total,con\ core} \times 10^{-6}/\pi} - \sqrt{A_{in,con\ core} \times 10^{-6}/\pi} & for\ outer\ concrete\ core \end{cases} \tag{4}$$

$$\alpha = \begin{cases} \left(2\sqrt{B^2 + H^2}\right) + 430 & for\ inner\ concrete\ core \\ \left(2\sqrt{B^2 + H^2}\right) + 580 & for\ outer\ concrete\ core \end{cases} \tag{5}$$

$$\beta = \begin{cases} 2\sqrt{\min(B, H)} & for\ inner\ concrete\ core \\ \dfrac{90}{\sqrt{B + H}} + 10.8 & for\ outer\ concrete\ core \end{cases} \tag{6}$$

$$M = 0.337 + 8.5\widetilde{t}_s + 30\widetilde{d}\left(\widetilde{d}^2 - 1.46\widetilde{d} + 0.64\right) \tag{7}$$

$$\widetilde{t_s} = \sqrt{A_{total,comp} \times 10^{-6}/\pi} - \sqrt{A_{total,con\ core} \times 10^{-6}/\pi} \tag{8}$$

$$C = \begin{cases} 2.1 & for\ inner\ concrete\ core \\ 1.2 & for\ outer\ concrete\ core \end{cases} \tag{9}$$

$$\alpha = \left(2\sqrt{B^2 + H^2}\right) + 656 \tag{10}$$

A comparison between finite element 2D result and empirical formula for the equivalent temperature vs. time of the concrete inner and outer core is plotted in Fig. 3. Fig. 3a–b shows the results for the 2C+2U section with a dimension of 153 mm × 153 mm, as a case example. For the 2C+2U-PE configuration, the result of a section (dimension of 153 mm × 89 mm) is presented in Fig. 3c–d. A good agreement is observed between equivalent temperature obtained from 2D heat transfer analysis and the empirical formulation.

A comparison between 2D finite element results and the empirical formulation for 74 cross-sections is presented in Fig. 4. The results show less than a 4% deviation in inner and outer concrete cores. This comparison shows the accuracy of the empirical formula for different cross-sections with various dimensions. The overall sections dimension is ranged from 89 mm × 153 mm–309 mm × 309 mm.

4.3. Steel equivalent temperature

The steel equivalent temperature is obtained from Eq. (2), where R is 575, C is 1.15, and M is a constant, calculated using Eq. (11) for non-embedded steel and related to the steel equivalent thickness.

$$M = 0.337 + 65\widetilde{t_s} \tag{11}$$

While for the embedded steel equivalent temperature, M is calculated from Eq. (12). L is the distance of the embedded steel surface to the section surface subjected to radiation (see Fig. 1), and $t_{s,emb}$ is the summation of all embedded steel plate thickness.

$$M = 0.337 + 0.0085t_{s,emb} + 30L\left(\left(L \times 10^{-3}\right)^2 - 0.00146L + 0.64\right) \tag{12}$$

A comparison between finite element 2D results and the empirical formula for the equivalent temperature vs. time of the steel

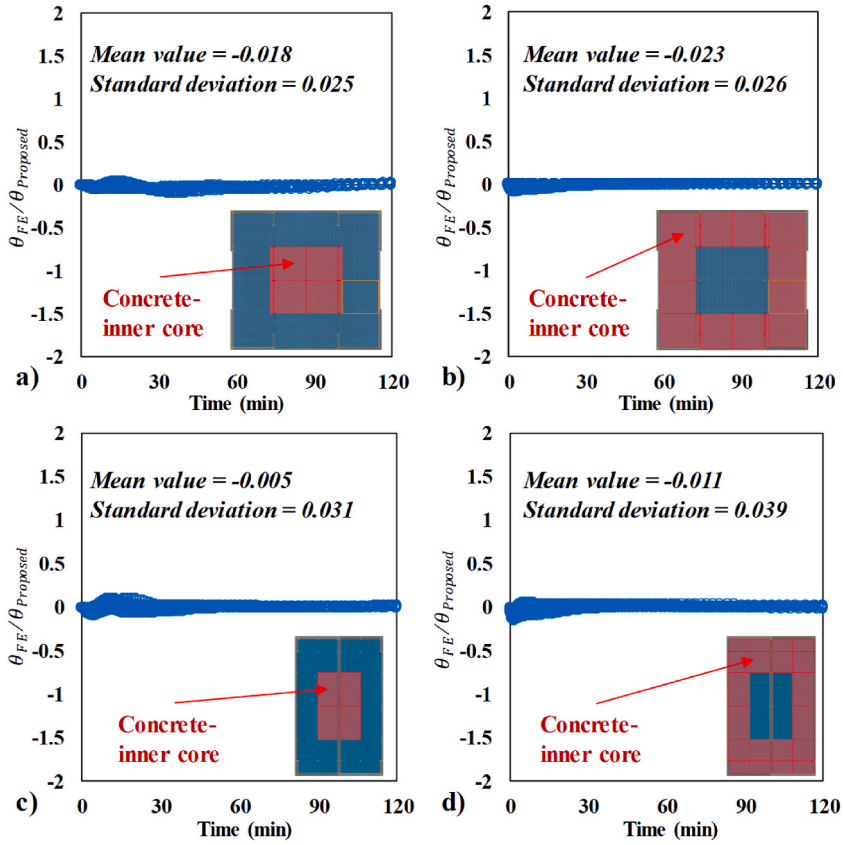

Fig. 4. Temperature history comparison for concrete; a) inner core (2C+2U) b) outer core (2C+2U), c) inner core (2C+2U-PE), and d) outer core (2C+2U-PE).

section is presented in Fig. 5. As a case example, Fig. 5a displays the findings for the 2C+2U section with a dimension of 153 mm × 153 mm, resulting in an excellent agreement (less than 5% differences). For the instance of 2C+2U-PE configuration, the outcome of a section (dimension of 153 mm × 89 mm) is illustrated in Fig. 5b–c. A good agreement is seen between the equivalent temperature derived from the 2D heat transfer study and the empirical formula for steel and embedded steel regions.

A comparison between 2D finite element results and the empirical formula for 74 cross-sections is provided in Fig. 6. The findings present less than a 4% deviation in steel and embedded steel area. This comparison illustrates the correctness of the empirical formula for several cross-sections with diverse section sizes.

4.4. Reliability analysis

Reliability analysis was undertaken for the proposed formulas by considering Cronbach's alpha (α), which is the most common test score in the reliability analysis. A Cronbach's alpha (α) higher than 0.7 was recommended as an acceptable value [33]. In this study, the Cronbach's alpha (α) values were consistently higher than 0.95, showing high similarity between the empirical formula and finite element methods.

5. Restriction on the formulae' applicability

The suggested empirical formulation for calculating the equivalent temperature may be used to analyze concrete-filled cold-formed steel (CF-CFS) built-up composite sections that meet the following criteria:

- CF-CFS composite cross-sections that individual CFS profiles are within the EN1993-1-3 [29] limitation for cold-formed profiles. The overall section dimension is ranged from 89 mm × 153 mm–309 mm × 309 mm. The high of the CFS profiles is ranged from 150 mm to 303 mm for C-shaped and from 153 mm to 309 mm for U-shaped. The width of the individual profiles also varies from 43 mm to 76.5 mm.
- Material thermal properties according to Part A [28].
- The heat transfer coefficient by convection is 25 W/m^2 K [31]. The resultant heat emissivity is 0.23 [16,28]].
- The fire exposure curve should be according to ISO 834 [32] and up to 2 h.

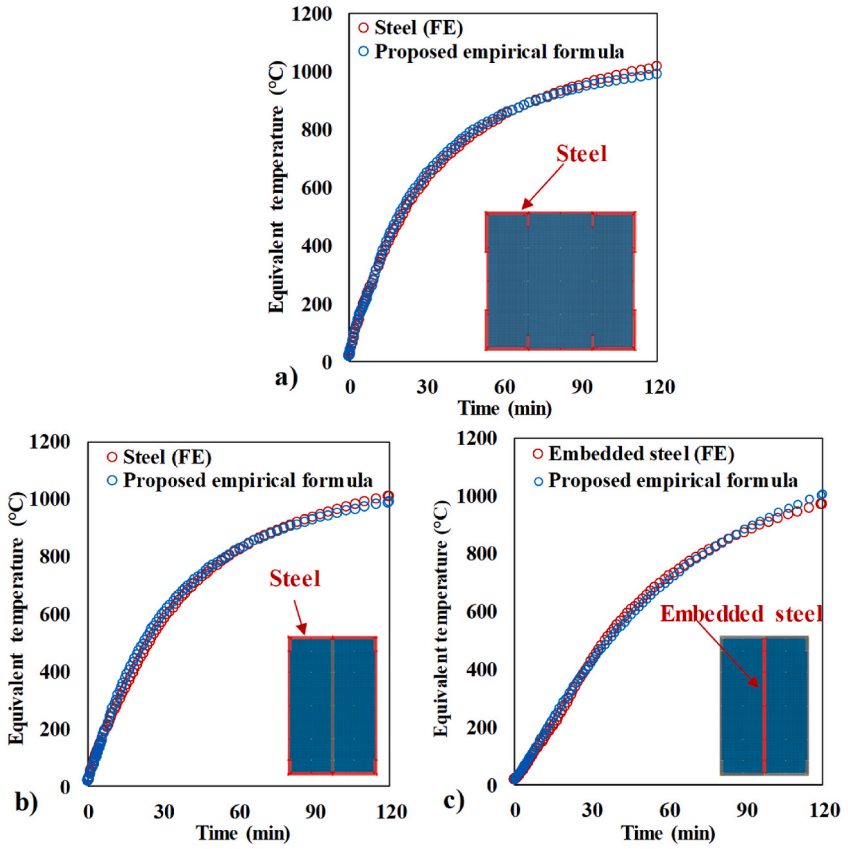

Fig. 5. Equivalent temperature history for steel; a) 2C+2U b) 2C+2U-PE, and c) embedded steel of 2C+2U-PE.

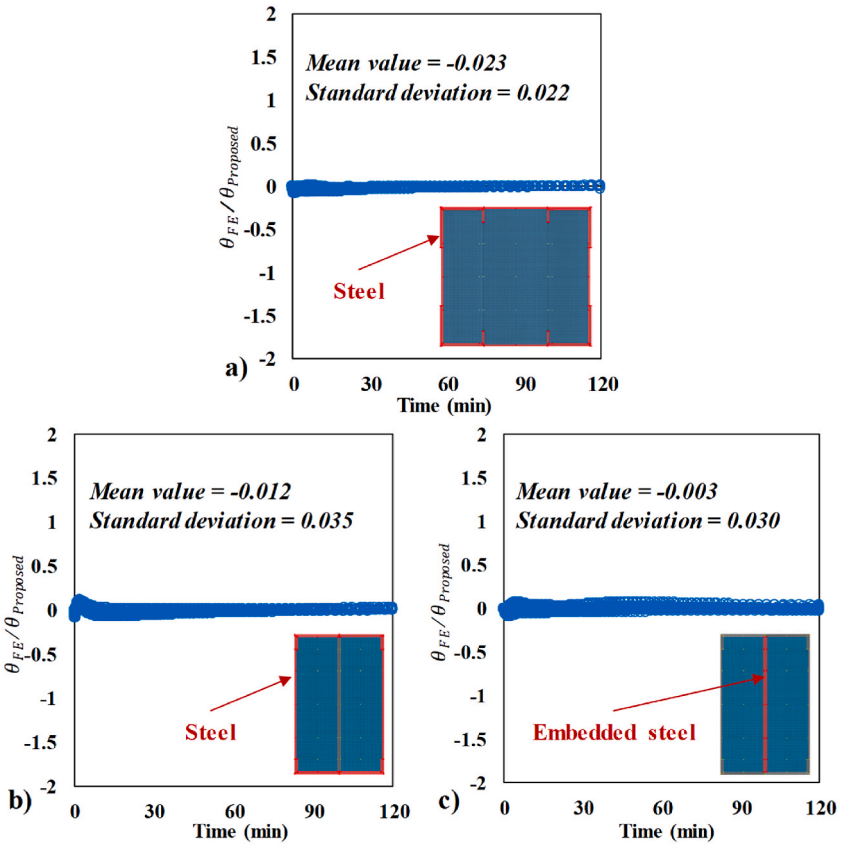

Fig. 6. Equivalent temperature history comparison for steel; a) 2C+2U b) 2C+2U-PE, and c) embedded steel of 2C+2U-PE.

6. Conclusions and future work

A 2D finite element modeling approach was presented and calibrated in Part A [28]. In this paper (Part B), a parametric study covered 74 CF-CFS cross-sections. Analyzing the heat transfer results, it was seen that the temperature deviation for the concrete-filled component is not remarkable from section center to the half dimension of the cross-section. Accordingly, a series of empirical formulas were proposed to predict the equivalent temperature for inner and outer concrete core, steel sections, and embedded steel area. The equivalent temperature results obtained from 2D finite element and empirical formulas were compared. The empirical formulas presented an accurate prediction compared to the 2D finite element results. Moreover, reliability analysis was undertaken considering Cronbach's alpha (α). The results represented the high reliability of the empirical formula. Further work is needed to extend the current formulation to cover various thermal properties and cross-section shapes.

CRediT authorship contribution statement

Rohola Rahnavard: Numerical modeling. Formulation. Formal analysis and interpretation of the results. Writing the original draft. Hélder D. Craveiro: Funding acquisition. Supervision. Formal analysis and interpretation of the results. Writing – review, and editing. Rui A. Simões: Supervision. Writing – review, and editing. Aldina Santiago: Writing – review, and editing.

Declaration of competing interest

The authors declared that there is no conflict of interest.

Acknowledgments

This work is financed by national funds through FCT - Foundation for Science and Technology, under grant agreement 2021.06528.BD attributed to the 1st author and under the grant agreement 2020.03588.CEECIND attributed to the 2nd author.

The authors gratefully acknowledge the Portuguese Foundation for Science and Technology (FCT) for its support under the framework of the research project PTDC/ECI-EGC/31858/2017 - INNOCFSCONC - Innovative hybrid structural solutions using cold-formed steel and lightweight concrete ", financed by FEDER funds through the Competitivity Factors Operational Programme-COMPETE and by national funds through FCT, and PCIF/AGT/0062/2018 – INTERFACESEGURA – Segurança e Resiliência ao Fogo

das Zonas e Interface Urbana-Florestal, financed by FCT through National funds.

This work was partly financed by FCT/MCTES through national funds (PIDDAC) under the R&D Unit Institute for Sustainability and Innovation in Structural Engineering (ISISE), under reference UIDB/04029/2020.

Appendix

A work example is presented to calculate the temperature for inner and outer concrete cores, steel, and embedded steel area. The 2C+2U-PE section with a dimension of 150 mm × 84 mm is selected. The thickness of each CFS profile is 1.5 mm.

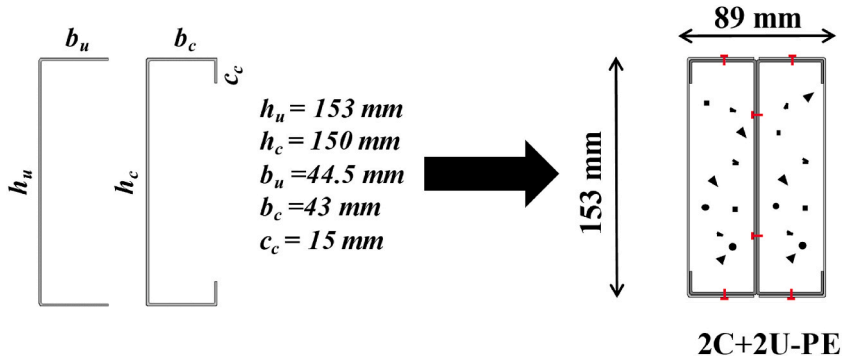

Figure A. Section dimension and details for work example.

For the inner concrete core, the following steps are needed:

$$\widetilde{d} = \sqrt{A_{in,con\ core} \times 10^{-6}/\pi} = \sqrt{2940 \times 10^{-6}/\pi} = 0.0306$$

$$\alpha = \left(2\sqrt{B^2 + H^2}\right) + 656 = \left(2\sqrt{189^2 + 153^2}\right) + 656 = 1010$$

$$\beta = 25$$

$$\widetilde{t}_s = \sqrt{A_{total,comp} \times 10^{-6}/\pi} - \sqrt{A_{total,con\ core} \times 10^{-6}/\pi} = \sqrt{13600 \times 10^{-6}/\pi} - \sqrt{12600 \times 10^{-6}/\pi} = 0.0025$$

$$R = 120 + \left(\alpha e^{-\beta \widetilde{d}}\right) = 120 + \left(1010 \times e^{-25 \times 0.0306}\right) = 590$$

$$M = 0.337 + 8.5\widetilde{t}_s + 30\widetilde{d}\left(\widetilde{d}^2 - 1.46\widetilde{d} + 0.64\right) = 0.905$$

Therefore, the equivalent temperature for the inner concrete core as a function of time is:

$$\theta_{eq,c} = 2R\left(1 - \frac{1}{1 + \left(t/M\right)^C}\right) + 20 = 1180\left(1 - \frac{1}{1 + \left(t/0.905\right)^{1.65}}\right) + 20$$

Accordingly, for the outer concrete core of the mentioned example, the equivalent temperature for the as a function of time is:

$$\theta_{eq,c} = 1352\left(1 - \frac{1}{1 + \left(t/0.918\right)^{1.2}}\right) + 20$$

For the steel, the equivalent temperature for the as a function of time is:

$$\theta_{eq,c} = 1150\left(1 - \frac{1}{1 + \left(t/0.49\right)^{1.2}}\right) + 20$$

For the embedded steel, the equivalent temperature for the as a function of time is:

$$\theta_{eq,c} = 1470\left(1 - \frac{1}{1 + \left(t/1.109\right)^{1.15}}\right) + 20$$

References

[1] Krishanu Roy, Tina Chui Huon Ting, Hieng Ho Lau, B. James, P. Lim, Nonlinear behaviour of back-to-back gapped built-up cold-formed steel channel sections under compression, J. Constr. Steel Res. 147 (2018) 257–276, https://doi.org/10.1016/j.jcsr.2018.04.007.

[2] Krishanu Roy, Mohammadjani Chia, B. James, P. Lim, Experimental and numerical investigation into the behaviour of face-to-face built-up cold-formed steel channel sections under compression, Thin-Walled Struct. 134 (2019) 291–309, https://doi.org/10.1016/j.tws.2018.09.045.

[3] Krishanu Roy, Tina Chui Huon Ting, Hieng Ho Lau, B. James, P. Lim, Experimental and numerical investigations on the axial capacity of cold-formed steel built-up box sections, J. Constr. Steel Res. 160 (2019) 411–427, https://doi.org/10.1016/j.jcsr.2019.05.038.

[4] Krishanu Roy, B. James, P. Lim, Hieng Ho Lau, P.M. Yong, G.C. Clifton, Ross P.D. Johnston, Andrzej Wrzesien, Chee Chiang Mei, Collapse behaviour of a fire engineering designed single-storey cold- formed steel building in severe fires, Thin-Walled Struct. 142 (2019) 340–357, https://doi.org/10.1016/j.tws.2019.04.046.

[5] Krishanu Roy, Boshan Chen, Zhiyuan Fang, Asraf Uzzaman, Xin Chen, B. James, P. Lim, Local and distortional buckling behaviour of back-to-back built-up aluminium alloy channel section columns, Thin-Walled Struct. 163 (2021), 107713, https://doi.org/10.1016/j.tws.2021.107713.

[6] Boshan Chen, Krishanu Roy, Asraf Uzzaman, Gary Raftery, B. James, P. Lim, Axial strength of back-to-back cold-formed steel channels with edge-stiffened holes, un-stiffened holes and plain webs, J. Constr. Steel Res. 174 (2020), 106313, https://doi.org/10.1016/j.jcsr.2020.106313.

[7] Krishanu Roy, Tina Chui Huon Ting, Hieng Ho Lau, B. James, P. Lim, Effect of thickness on the behaviour of axially loaded back-to-back cold-formed steel built-up channel sections - experimental and numerical investigation, Structures 16 (2018) 327–346, https://doi.org/10.1016/j.istruc.2018.09.009.

[8] B. Young, J. Chen, Design of cold-formed steel built-up closed sections with intermediate stiffeners, J. Struct. Eng. 134 (5) (2008) 727–737.

[9] J.H. Zhang, B. Young, Finite element analysis and design of cold-formed steel built-up closed section columns with web stiffeners, Thin-Walled Struct. 131 (2018) 223–237.

[10] Sivaganesh Selvaraj, Mahendrakumar Madhavan, Design of cold-formed steel built-up closed section columns using direct strength method, Thin-Walled Struct. 171 (2022), 108746, https://doi.org/10.1016/j.tws.2021.108746.

[11] Sivaganesh Selvaraj, Mahendrakumar Madhavan, Design of cold-formed steel built-up columns subjected to local-global interactive buckling using direct strength method, Thin-Walled Struct. 159 (2021), 107305, https://doi.org/10.1016/j.tws.2020.107305.

[12] S. Gunalan, D. Bandula Heva, M. Mahendran, Cold-formed steel columns subject to local buckling at elevated temperatures, in: Proceedings of the Steel Innovations Conference 2013, Steel Construction New Zealand, 2013, pp. 1–10.

[13] Sivaganesh Selvaraj, Mahendrakumar Madhavan, Structural design of cold-formed steel face-to-face connected built-up beams using direct strength method, J. Constr. Steel Res. 160 (2019) 613–628, https://doi.org/10.1016/j.jcsr.2019.05.053.

[14] Liping Wang, Ben Young, Behaviour and design of cold-formed steel built-up section beams with different screw arrangements, Thin-Walled Struct. 131 (2018) 16–32, https://doi.org/10.1016/j.tws.2018.06.022.

[15] H.D. Craveiro, R. Rahnavard, J. Henriques, R.A. Simões, Structural fire performance of concrete-filled built-up cold-formed steel columns, Materials 15 (2022) 2159, https://doi.org/10.3390/ma15062159.

[16] Rohola Rahnavard, Hélder D. Craveiro, Rui A. Simões, Luís Laím, Aldina Santiago, Fire resistance of concrete-filled cold-formed steel (CF-CFS) built-up short columns, J. Build. Eng. (2021), 103854, https://doi.org/10.1016/j.jobe.2021.103854.

[17] Rohola Rahnavard, Hélder D. Craveiro, Rui A. Simões, Luís Laím, Aldina Santiago, Buckling resistance of concrete-filled cold-formed steel (CF-CFS) built-up short columns under compression, Thin-Walled Struct. 170 (2022), 108638, https://doi.org/10.1016/j.tws.2021.108638.

[18] T.T. Lie, R.J. Irwin, Fire resistance of rectangular steel columns filled with bar-reinforced concrete, J. Struct. Eng. 121 (Issue 5) (1994), https://doi.org/10.1061/(ASCE)0733-9445 (1995)121:5(797).

[19] Kingsley U. Ukanwa, Umesh Sharma, Stephen J. Hicks, Anthony Abu, B. James, P. Lim, G. Charles Clifton, Behaviour of continuous concrete filled steel tubular columns loaded concentrically in fire, J. Constr. Steel Res. 136 (2017) 101–109, https://doi.org/10.1016/j.jcsr.2017.05.011.

[20] Kingsley U. Ukanwa, James B.P. Lim, Umesh K. Sharma, Stephen J. Hicks, Anthony Abu, G. Charles Clifton, Behaviour of continuous concrete filled steel tubular columns loaded eccentrically in fire, J. Constr. Steel Res. 139 (2017) 280–287, https://doi.org/10.1016/j.jcsr.2017.09.030.

[21] Kingsley U. Ukanwa, G. Charles Clifton, James B.P. Lim, Stephen J. Hicks, Umesh Sharma, Anthony Abu, Simple design procedure for concrete filled steel tubular columns in fire, Eng. Struct. 155 (2018) 144–156, https://doi.org/10.1016/j.engstruct.2017.10.062.

[22] Kingsley U. Ukanwa, G. Charles Clifton, James B.P. Lim, Stephen J. Hicks, Umesh Sharma, Anthony Abu, Design of a continuous concrete filled steel tubular column in fire, Thin-Walled Struct. 131 (2018) 192–204, https://doi.org/10.1016/j.tws.2018.07.001.

[23] Min Yu, Haoming Xu, Jianqiao Ye, Chi Yin, A unified interaction equation for strength and global stability of solid and hollow concrete-filled steel tube columns under room and elevated temperatures, J. Constr. Steel Res. 148 (2018) 304–313, https://doi.org/10.1016/j.jcsr.2018.05.026.

[24] Min Yu, Xiaoxiong Zha, Jianqiao Ye, Baolin Wang, A unified method for calculating fire resistance of solid and hollow concrete-filled steel tube columns based on average temperature, Eng. Struct. 71 (2014) 12–22, https://doi.org/10.1016/j.engstruct.2014.03.038.

[25] Min Yu, Wang Tan, Weijun Huang, Huanxin Yuan, Jianqiao Ye, Fire resistance of concrete-filled steel tube columns with preload, Part I: Exp. Invest. Compos. Struct. 223 (2019), 110994, https://doi.org/10.1016/j.compstruct.2019.110994.

[26] Min Yu, Wang Tan, Weijun Huang, Jianqiao Ye, Fire resistance of concrete-filled steel tube columns with preload. Part II: numerical and analytical investigation, Compos. Struct. 223 (2019), 110995, https://doi.org/10.1016/j.compstruct.2019.110995.

[27] Design of Steel and Composite Structures, Part 1.2: Structural Fire Design. ENV 1994-1-2, British Standards Institution: European Committee for Standardization, London, 2003.

[28] Rohola Rahnavard, Hélder D. Craveiro, Rui A. Simões, Aldina Santiago, Equivalent temperature prediction for concrete-filled cold-formed steel (CF-CFS) built-up column sections (part A), Case Stud. Therm. Eng. 33 (2022), 101928, https://doi.org/10.1016/j.csite.2022.101928.

[29] EN 1993-1-3 (2006) (English): Eurocode 3: Design of Steel Structures - Part 1-3: General Rules - Supplementary Rules for Cold-Formed Members and Sheeting.

[30] Abaqus [61] Analysis User's Guide, Version 6.17 Dassault Systèmes Simulia USA, 2017.

[31] EN 1991-1-2 (2002) (English): Eurocode 1: Actions on Structures - Part 1-2: General Actions - Actions on Structures Exposed to Fire.

[32] ISO 834-1, Fire-Resistance Tests—Elements of Building Construction—Part 1: General Requirements, International Standard ISO, Geneva, 1999.

[33] J. Bland, D. Altman, Statistics notes: Cronbach's alpha, BMJ 314 (1997) 275, https://doi.org/10.1136/bmj.314.7080.572.